Reprinted from the Twenty-Seventh
International Conference on Coastal Engineering
Coastal Eng. Res. Council - ASCE
July 16-21 2000 - Sydney, Australia

3-D MODELING OF RIP CURRENTS

Kevin A. Haas, Ib A. Svendsen and Qun Zhao [1]

Abstract

The present paper describes the 3-D variation of rip currents through the use of physical and numerical models. Experimental measurements of rip currents are made in a directional wave basin. The vertical profile of the rip current is found to vary from depth uniform inside the channel to depth varying further offshore. Offshore from the channel the rip current has much stronger velocities at the surface than near the bottom. A nearshore circulation numerical modeling system is applied to the wave basin. The results from the model show qualitative and quantitative agreement with the laboratory measurements.

Introduction

In the literature, such as Sonu (1972) and Shepard and Inman (1950), indications are that although rip currents appear to be depth uniform inside the surf zone, outside the breakers, rip currents tend to become surface currents. Predicting where and when a rip current occurs is difficult, thereby making measurements of rip currents in the field a difficult task. When measurements of rip currents are made in a controlled laboratory environment, predicting the location of rip currents becomes trivial. This paper presents laboratory measurements that extend the experiments performed by Haller *et al.* (1997a,b) to include information about the current variation over depth.

In addition, numerical modeling of the rip current system is presented. Historically, numerical nearshore circulation models have been 2-D utilizing depth-averaged currents. More recently models have been including the effects of the vertical variation of the currents forming the so-called quasi 3-D models. The vertical variation of the horizontal velocities leads to mixing like terms which augment other lateral mixing mechanisms such as turbulence. The SHORECIRC (SC) modeling system (version 2.0, described by Haas and Svendsen (2000)) has previously been tested for simulating rip currents by Haas *et al.* (1998) and is used here to model the vertical variation of the rip currents.

Physical modeling

[1]Center for Applied Coastal Research, Ocean Engineering Lab, University of Delaware, Newark, DE 19716, USA. Correspondence e-mail: haas@coastal.udel.edu

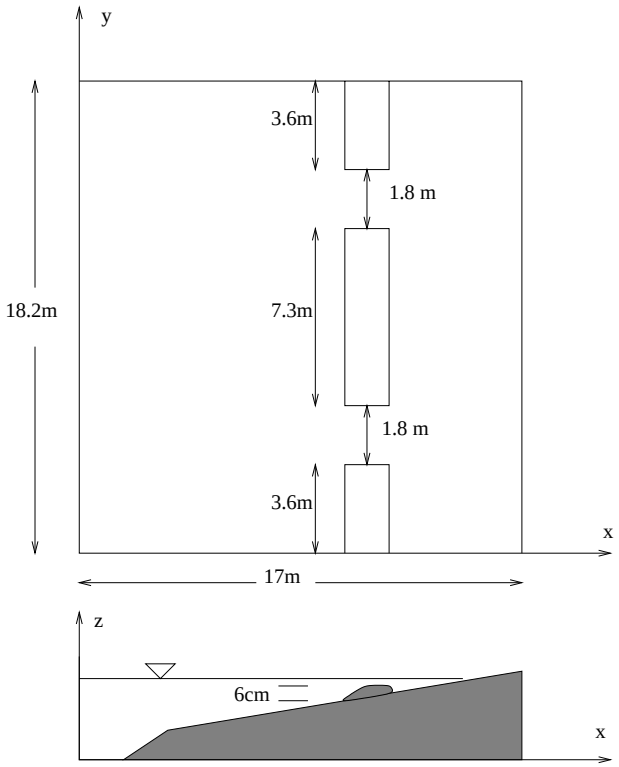

Figure 1: Design Topography.

The laboratory experiment is performed in the directional wave basin located in the Ocean Engineering Laboratory at the University of Delaware. The design view of the wave basin is seen in Figure 1. The waves are created by a snake-type wave maker located at the toe of a steep 1:5 slope preceding a milder 1:30 slope. A longshore bar of height 6 cm with two channels is centered about 11.8 m from the offshore wall and the two channels are approximately 1.8 m wide.

The original experiments by Haller and Dalrymple (1999) primarily focus on obtaining information about a horizontal spatial overview of the rip current circulation pattern. At most locations, measurements are only available for one depth which is selected to give a good representation of the depth-averaged currents. The time-averaged velocity vectors from these experiments are seen in Figure 2(a). The measurements span a large portion of the wave basin, providing a good spatial overview of the rip current system. The primary focus lies within the rip channel, indicated by the dense number of measurements within the channel.

The present measurements are focused inside and offshore of the rip channel in order to learn about the evolution of the rip as it flows offshore. The purpose of the experiments particularly is to gain understanding of the vertical variation of the rip currents. In addition, information is obtained about the temporal variation for the vertical profiles of rip currents.

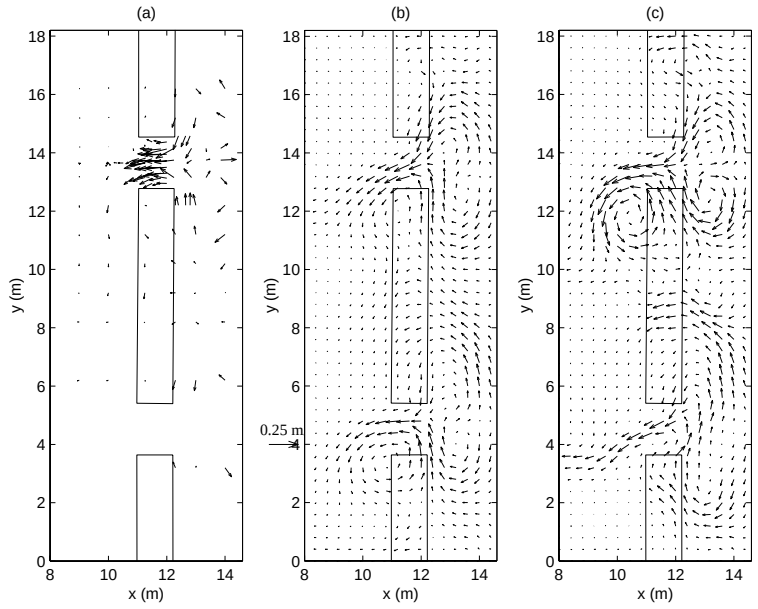

Figure 2: Time-averaged velocity vectors from (a) Haller *et al.* (1997a,b) and (b) SHORECIRC. (c) shows instantaneous velocity vectors for an arbitrary time from the SHORECIRC simulation.

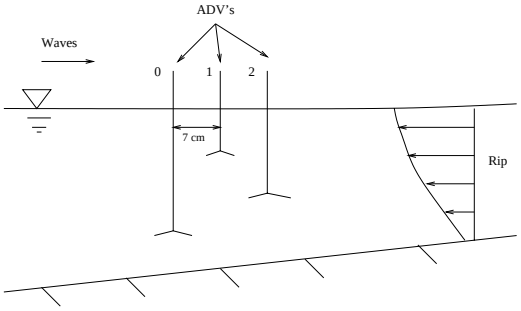

Figure 3: Setup for the ADV's.

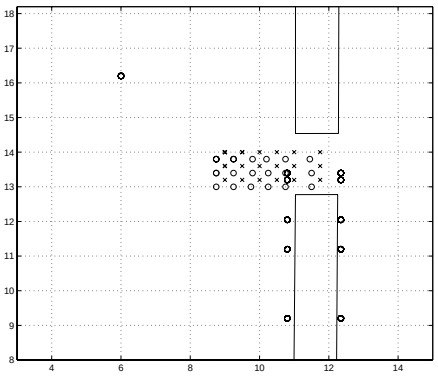

Figure 4: Location of the gages for Test R where (x) indicates ADV gage array locations and (o) indicates wave gage locations.

Three Sontek Acoustic Doppler Velocimeters (ADV's) are used for measuring the velocities. The three ADV's are side-looking two-dimensional probes. The ADV's are mounted on a movable carriage in an arrangement indicated in Figure 3 such that they are as close to each other as possible (7 cm). In order to measure the depth variation of the current, the probes are put at three different depths. The offshore gage (ADV 0) is placed near the bottom, the middle gage (ADV 1) is placed near the surface just below the trough level of the waves and the shoreward gage (ADV 2) is placed close to mid-depth. The measurements from the three gages are used together to provide a vertical profile of the current taken at the location of ADV 1.

The locations of the measurements for Test R are shown in Figure 4. Each (x) in the figure represents the location of the ADV array comprised of the three ADV's as previously described. Each (x) on Figure 4 represents individual runs of the same experiment. The ADV arrays are located along 3 separate cross-shore lines containing 6 measurements each resulting in 18 total runs. This covers a broad region within and seaward of the channel.

The circles (o) in Figure 4 represent individual wave gages. One wave gage is always located offshore ($x = 6$ m, $y = 16.2$ m) and is used to check repeatability of the experiments. In order to provide water level data close to the current measurements, another wave gage is always placed close to the ADV array. Finally, 5 wave gages are placed on a bridge spanning the longshore direction which is located shoreward of the bar for half of the runs and seaward of bar for the rest of the runs.

The velocity time series is low-pass filtered to remove the short-wave oscillations. The low-pass filtered cross-shore velocity time series, measured close to the water surface, is shown in Figure 5 for three cross-shore locations along the centerline of the channel. In addition, a line indicating the mean value of the current, averaged over the entire time series, is drawn on each plot (negative velocity

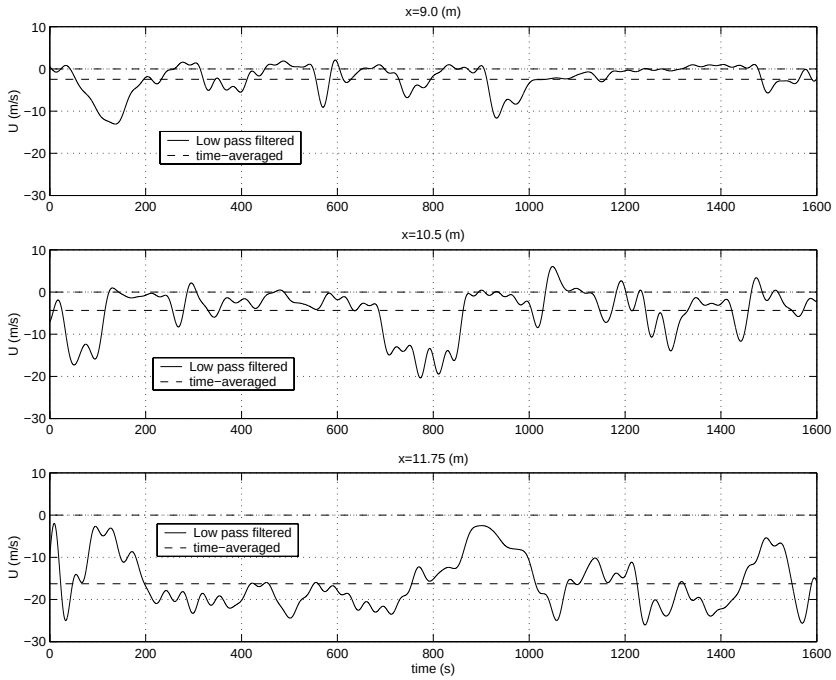

Figure 5: Low-pass filtered velocity time series with the long-term time-average along the centerline of the channel. The top panel is run R17 ($x = 9$ m), the middle panel is run R6 ($x = 10.5$ m) and the bottom panel is R8 ($x = 11.75$ m)

indicates an offshore flow). As suggested by the instantaneous flow pattern shown in Figure 2(c), the flow varies significantly with time.

The offshore ($x = 9$ m) rip only occurs sporadically in the top panel, therefore, the mean value of the velocity when averaged over the entire time period is small. The mean velocity is around 2 cm/s whereas the peak velocity in the rip reaches as high as 12 cm/s. This helps to explain why the time-averaged rip in Figure 2(a) appears to vanish offshore. The middle panel continues to show sporadic rip events although more frequently than the top panel. Again, the mean velocity is small, reaching a value of 4 cm/s with the peak velocity being much larger, around 20 cm/s. Only the time series in the middle of the channel ($x = 11.75$ m) has a mean velocity which is representative of the rip. The mean value is around 17 cm/s and the peak rip is about 25 cm/s.

Figure 6 shows the cross-shore and longshore low pass filtered velocities for all three depths measured at the centerline of the channel, offshore of the bar at $x = 9$ m. In Figure 6, strong depth variations clearly exist in the cross-shore velocity. For example, around $t = 950$ seconds there is a strong rip occurrence. The velocity closest to the surface is large, around 12 cm/s, but at mid-depth, the velocity is smaller, only around 4 cm/s. Yet, close to the bottom, the velocity is approximately 2 cm/s and is directed shoreward. The trend of shoreward velocity at the bottom continues throughout most of the time series, with only a few

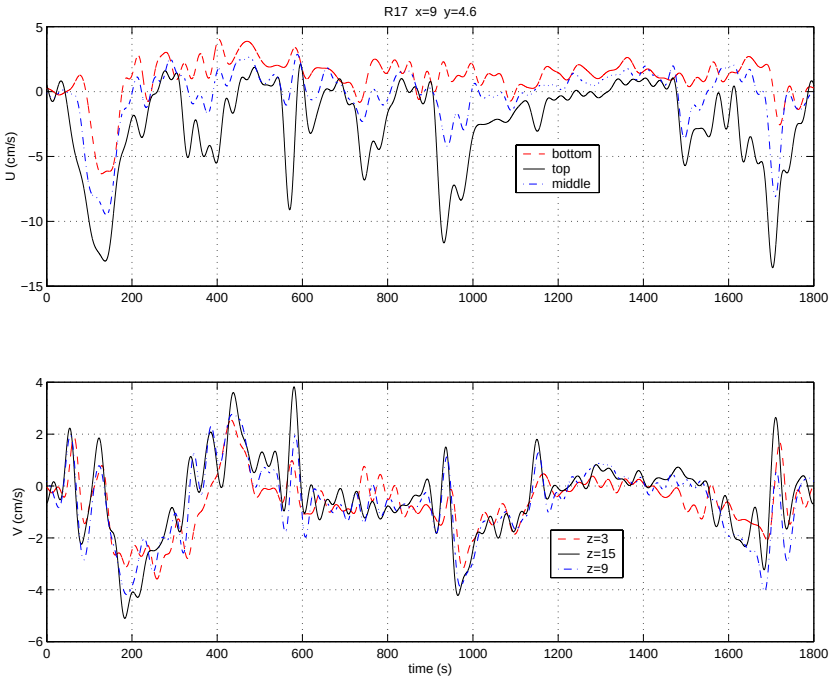

Figure 6: Low-pass filtered velocity time series at three depths for run R17 ($x = 9$ m). The top panel is cross-shore velocities (U) and bottom panel is longshore velocities (V).

exceptions of offshore flow. Throughout this time series, at the offshore points the cross-shore velocity in the rip rarely penetrates to the bottom of the water column. On the other hand, the longshore velocity in the bottom panel of Figure 6 demonstrates fairly depth uniform behavior. This eliminates the possibility of flow separation, because when flow separates from the bottom there should be similar depth variation in both the cross-shore and longshore velocities.

Similarly, Figure 7 shows the low-pass filtered velocities inside the surfzone at $x = 11.75$ m. The cross-shore velocities inside the channel shown in the top panel of Figure 7 clearly indicate depth uniform flow. More depth variation occurs in the longshore flow shown in the bottom panel than in the cross-shore flow. In addition, the magnitude of the longshore current is similar to the magnitude of the cross-shore current.

The depth variation also gives another reason for why the rip current vanishes shortly offshore of the channel in Figure 2(a). Most of the measurements used to generate the velocity vectors in this figure were taken at mid-depth or lower. As seen in Figure 6, measurements at mid-depth or lower offshore of the channel have much lower velocities than the measurements taken close to the surface. This leads to the conclusion that the rip doesn't necessarily vanish as it flows offshore, it passes over the top of the gages located lower in the water column. It should be noted that the focus of the study by Haller and Dalrymple (1999) is on the

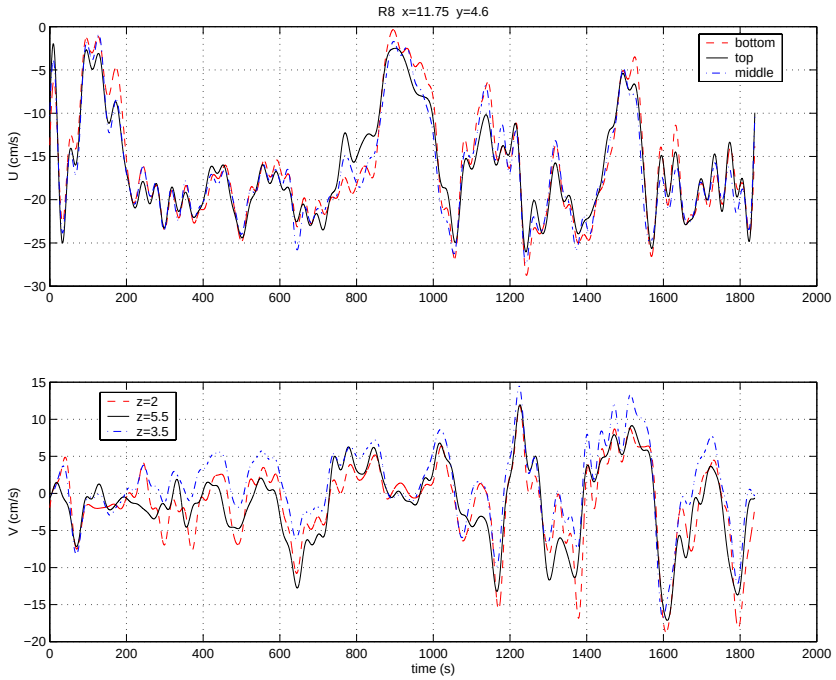

Figure 7: Low-pass filtered velocity time series at three depths for run R8 ($x = 11.75\,\mathrm{m}$). The top panel is cross-shore velocities (U) and bottom panel is longshore velocities (V).

rip velocities in the channel, where, as indicated in Figure 7, the velocities are nearly uniform over depth so that measurements lower in the water column are representative of the velocity over all depths.

The velocities are measured at each horizontal location during different runs which prevents direct comparisons between the time series. In addition the rip behavior is not identical between runs, i.e. even measurements at the same location for separate runs are different. The repeatable aspect of the experiments is the time-averaged properties and not the instantaneous flow pattern. In addition, as previously mentioned, time-averaging the velocity records over the length of the experiments annihilate the rip signal outside the surfzone.

In order to analyze the cross-shore variation of the rip current profiles a bin-averaging technique is utilized. The velocity profiles are sorted into bins based on the magnitude of the cross-shore velocity measured closest to the surface (U_1). The bins are defined using the following criteria,

$$\begin{aligned} &\text{if} \quad U_1 > 25 \quad &&\text{bin25} \\ &\text{if} \quad 25 > U_1 > 20 \quad &&\text{bin20} \\ &\text{if} \quad 20 > U_1 > 15 \quad &&\text{bin15} \\ &\text{if} \quad 15 > U_1 > 10 \quad &&\text{bin10}. \end{aligned}$$

The velocity profiles are averaged within each bin producing four velocity profiles,

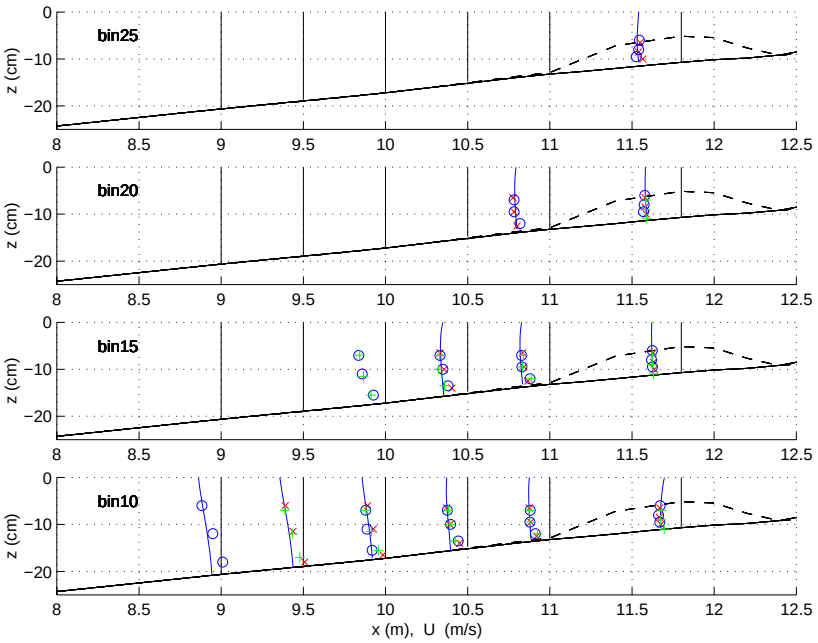

Figure 8: Bin-averaged rip current profiles, from top to bottom, bin25, bin20, bin15 and bin10. The symbols are defined as (x) - $y = 13.2$, (o) - $y = 13.6$ and (+) - $y = 14.0$ and the solid line is the profile calculated from SC. The vertical lines are the reference lines for each location.

one for each bin. The bin averaging is done at each measurement location allowing for direct comparisons between the velocity profiles at different locations.

Figure 8 shows the velocity profiles for each bin at all of the locations. The cross-shore velocity near the surface does not meet the criteria for the bins at all the locations, which explains the absence of many profiles, especially for bin25 in the top panel. The three profiles at any given cross-shore location show little variation implying that regardless of where the rip passes in the longshore direction, the vertical profile of the rip remains unchanged. Measurements at different longshore locations within the region where the rip passes produce the same velocity profile whenever the rip is present, therefore, further experiments will focus primarily on one cross-shore section, along the centerline of the channel.

The transition of the depth variation is evident, particularly in bin10. Inside the channel the velocity is virtually depth uniform whereas the velocity exhibits strong depth variations farther offshore. Keep in mind that the profiles represent the bin-averaged velocity and are not an indication of the instantaneous depth variations. Therefore, the bottom panel in Figure 8 does not represent the actual instantaneous depth variation of a rip current flowing off shore.

Variations of the velocity profiles in time can be compared at any given location. Because the gages are offset by 7 cm in the cross-shore direction, the

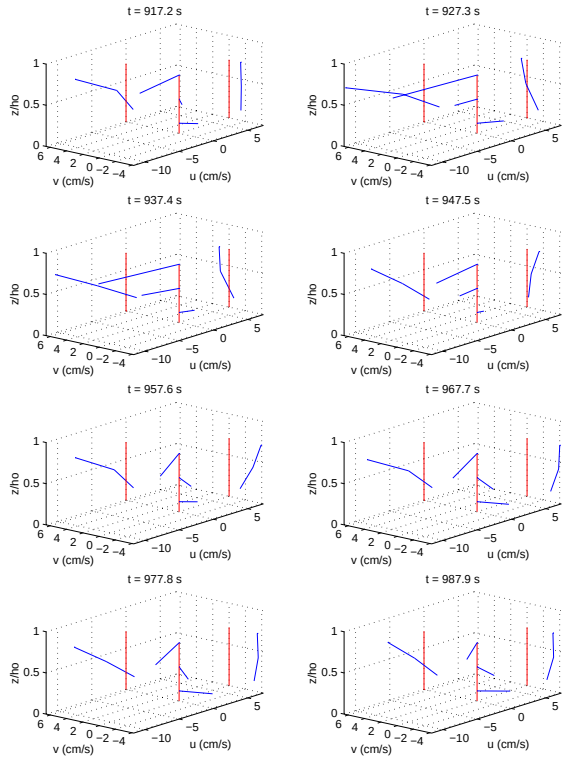

Figure 9: Snapshots of the vertical profiles of velocity for run R17 ($x = 9$ m).

measurements contain some phase shift between the different depths. For this reason, instantaneous profiles are calculated by averaging the low-pass filtered velocity over 5 seconds. This time scale is much shorter than the time variations of the rip flow, therefore, little information is lost from the averaging process.

Vertical profiles of velocity from eight times during a rip event at the location 2 m offshore of the bar are shown in Figure 9. The vertical lines are the reference lines. The horizontal lines are vectors indicating both the magnitude and direction of the current. The projections of the cross-shore and longshore velocities are included as well. The largest offshore (negative) current is located at the top whereas the weakest or onshore (positive) current is at the bottom. The cross-shore velocities exhibit the strong depth variations but the longshore velocity remains fairly depth uniform. The current is twisting over depth with the surface velocity going mainly offshore and the bottom current going in the negative longshore direction and slightly shoreward.

In contrast, Figure 10 shows vertical profiles of velocity at eight times during a rip event inside the channel. Here the vertical profiles tend to be depth uniform with little twisting of the current evident. During the initial surge of the rip, the peak current is occurring at mid-depth, although as the velocity reduces, the peak tends to move towards the surface.

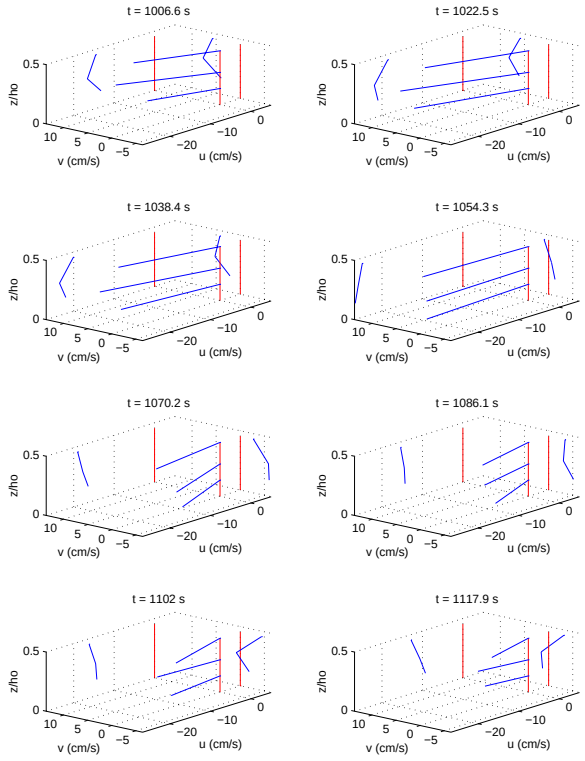

Figure 10: Snapshots of the vertical profiles of velocity for run R8 ($x = 11.75$ m).

Numerical Modeling

The topography and wave conditions for the experiments in the CACR wave basin are used in SC to model the rip currents. A qualitative comparison between the depth-averaged velocity from SC and the laboratory measurements can be seen in Figure 2(b). Quantitative comparisons of depth-averaged properties to the experimental measurements are given by Haas *et al.* (1998).

The modeling is done for the conditions of Test R from the previous section which corresponds to Test B from Haller and Dalrymple (1999) This allows for direct comparisons between vertical profiles calculated by the numerical model and the experimental measurements. A simple time-average is ineffective because it suppresses the rip signal due to the sporadic nature of the rip, therefore, the bin averaging method from the previous section is utilized.

Time series of velocity profiles are calculated at the same locations as the experimental measurements. The current is sorted into the bins based on the velocity at the same depth as the measurement from the gage closest to the surface. This is the identical sorting method used on the experimental measurements, allowing direct comparisons. The current is averaged to produce vertical profiles in each bin for all of the cross-shore locations.

The bin-averaged profiles are shown in Figure 8 along with the bin-averaged

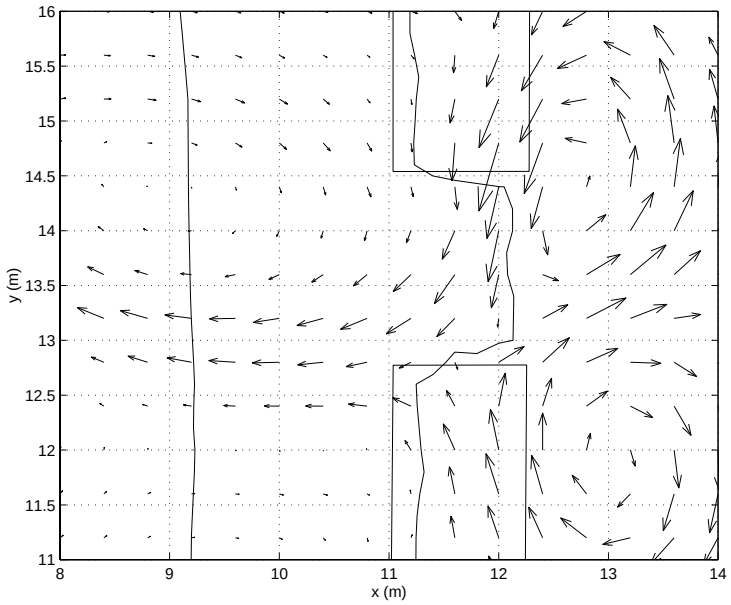

Figure 11: Instantaneous snapshot of $V_{m\alpha}$ vectors and topography contours for a different time than Figure 2c focusing on one rip current.

measurements. The modeled profiles are quite similar to the measurements, fairly depth uniform in the channel and stronger depth variations offshore with increased velocity near the surface. In addition, the modeled profiles appear in nearly all of the same bins as the measurements at each location. This is an indication that the relative strength of the modeled rip current is similar to the strength of the actual rip current in the basin.

Inside the channel the modeled currents and measurements are in excellent agreement. Farther offshore the agreement is good at the upper and mid-depth locations. In bin10 at the farthest location offshore, the velocity close to the surface is in good agreement but the velocity at the bottom is slightly over-predicted. In general, this trend holds true and the velocity near the bottom is slightly over-predicted for most locations outside the surfzone.

The advantage of using a numerical model is that the model provides the currents over the entire domain simultaneously. Figure 11 provides an instantaneous vector plot of the depth-averaged velocity $V_{m\alpha}$ for a time when a strong rip is flowing offshore. The rip is not flowing through the center of the channel, rather it is flowing out of the side of the channel. Note that this figure only shows an excerpt of the entire computational domain and in order to reduce clutter the vectors are not plotted at every computational point.

Figure 12 shows the computed results for the three-dimensional variation of the currents in and around the channel. The center row of profiles shows the depth variation of the current through the center of the rip current. The two rows

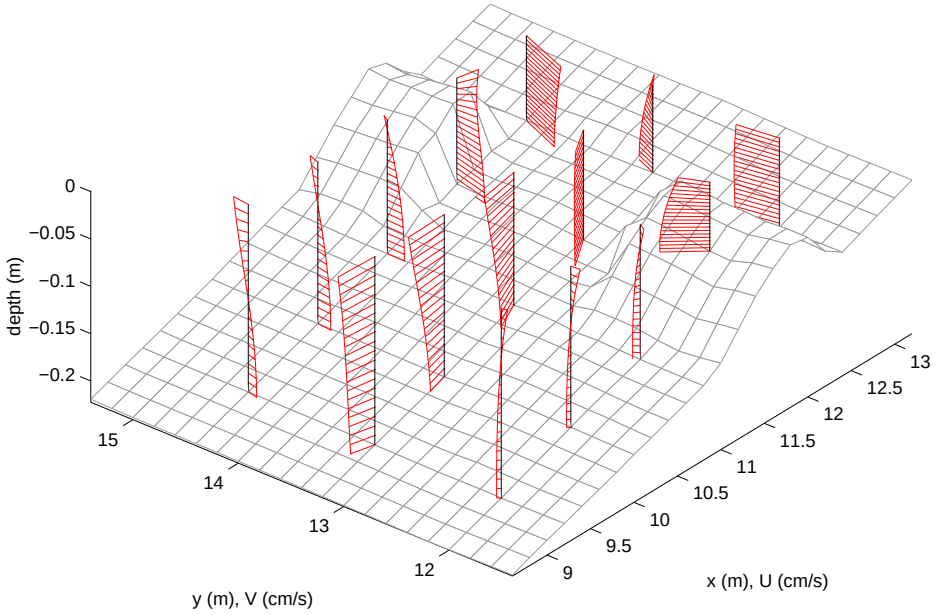

Figure 12: Instantaneous snapshot of the 3D variation of V_α centered along the middle of the rip current for the flow pattern from Figure 11.

of profiles on the sides show the feeder currents. The rip shows significant depth variations, larger velocity at the surface than the bottom as the rip flows offshore but the feeder currents behind and over the bar have little depth variation. The profiles along the edge of the rip offshore of the bar have currents at the surface flowing away from the rip. Even though the currents along $y = 14.4$ m are feeding the rip, the velocity at the surface is away from the rip.

The time evolution of the vertical variations of currents are shown in Figures 13 and 14. Each of these figures show eight three-dimensional snapshots of the vertical variation of the current during a burst of the rip current. These figures are similar to the three-dimensional plots of the measurements shown in Figures 9 and 10.

Figure 13 shows the currents at $x = 9, y = 13.6$ m which is 2 m offshore from the bar. This figure is for the same location as the profiles of measurements in Figure 9. Initially there is little depth variation but as the burst of rip velocity grows, the depth variation becomes significant. The velocity at the surface is much larger than the velocity at the bottom. In the later stages, the velocity at the bottom becomes slightly shoreward even though the velocity in the upper part of the water column is offshore. The vertical variation of the rip in this figure is qualitatively similar to the vertical variation of the rip current from the measurements in Figure 9.

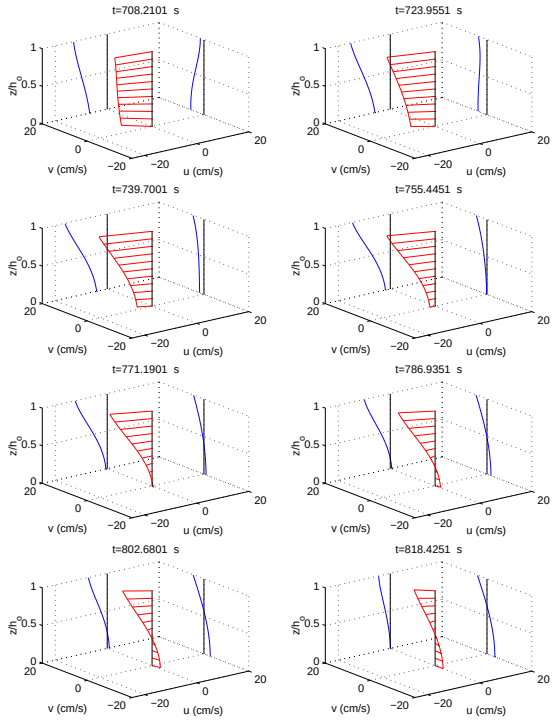

Figure 13: Snapshots in time of the vertical variation of V_α at $x = 9$ m.

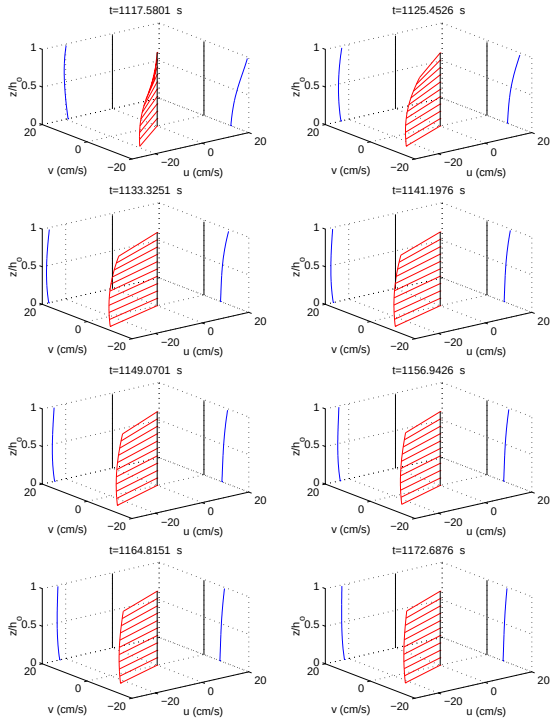

Figure 14: Snapshots in time of the vertical variation of V_α at $x = 11.8$ m.

Finally, Figure 14 shows the vertical profiles for the rip in the middle of the channel at $x = 11.8, y = 13.6$. The cross-shore profiles show slight curvature reducing the velocity near the surface. The longshore currents are only slightly weaker than the cross-shore currents indicating that the rip is not flowing straight offshore but at a small angle through the channel.

Conclusions

The laboratory measurements of the rip currents demonstrate the vertical structure of the rips inside and outside the surfzone. Inside the surfzone the currents tend to be close to depth uniform with a slightly reduced velocity close to the surface. Contrarily, the currents outside the surfzone have significant depth variations with strong offshore velocities near the surface and weak offshore or even shoreward velocities near the bottom. In addition, the measurements show that the cross-shore currents inside the rip have the same vertical profile regardless of the longshore position of the rip.

The nearshore circulation model SHORECIRC is used to simulate the rip currents in the wave basin. Good agreement between the measurements and model results is achieved which makes it possible to analyze the rip current structure in more detail.

Both the experiments and model show that at fixed points rip currents appear sporadic in nature. Though flowing all the time, the instabilities cause the rip current to appear at a given offshore point infrequently. Long-term time-averaging makes the rip current appear to vanish just outside of the channel even though instantaneously the rip flows much farther offshore.

Acknowledgements

This work was sponsored by Sea Grant, under Award No R/OE-26 and by ONR (contract no N0014-99-1-0291). The US government is authorized to produce and distribute reprints for government purposes not withstanding any copyright notation that may appear herein.

References

Haas, K., Svendsen, I., and Haller, M. (1998). Numerical modeling of nearshore circulation on a barred beach with rip channels. In *Proc. 26th Coastal Engineering Conference*, volume 1, pages 801–814, Copenhagen. ASCE.

Haas, K. A. and Svendsen, I. A. (2000). Three-dimensional modeling of rip current systems. In preparation.

Haller, M. and Dalrymple, R. A. (1999). Rip current dynamics and nearshore circulation. (Ph. D. Dissertation), Res. Report CACR-99-05, Center for Applied Coastal Research, Univ. of Delaware.

Haller, M., Dalrymple, R., and Svendsen, I. (1997a). Rip channels and nearshore circulation: Experiments. In *Proceedings Coastal Dynamics*, pages 594–603.

Haller, M., Dalrymple, R., and Svendsen, I. (1997b). Experimental modeling of a rip current system. In *Proceedings of the Third International Symposium on Ocean Wave Measurement and Analysis*.

Shepard, F. P. and Inman, D. L. (1950). Nearshore water circulation related to bottom topography and wave refraction. *Transactions, American Geophysical Union*, **31**, 196–212.

Sonu, C. J. (1972). Field observations of nearshore circulation and meandering currents. *Journal of Geophysical Research*, **77**, 3232–3247.